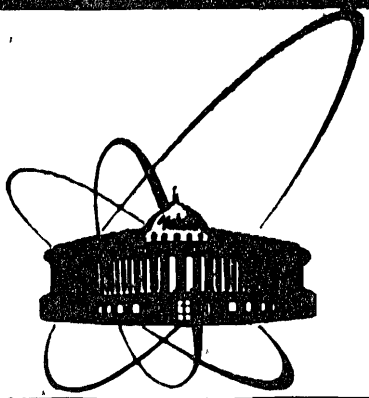

сообщения
объединенного
института
ядерных
исследований
дубна

E13-87-388

Gy.L.Bencze, L.M.Soroko

IMAGING PROPERTIES OF THE MESOOPTICAL FOURIER TRANSFORM MICROSCOPE FOR NUCLEAR RESEARCH EMULSION

1987

1. INTRODUCTION

The Mesooptical Fourier Transform Microscope (MFTM) for nuclear research emulsion is described in [1-7]. The purpose of the MFTM is to observe selectively only straight line particle tracks in a thick nuclear emulsion layer and by means of a proper computing algorithm which has been mentioned in [6] to find events-nuclear interactions. These interactions are seen as star-like patterns consisting of several straight line particle tracks which start from a common vertex. The MFTM enables us to find events the vertex of which is outside the field of view of the MFTM.

In the previuos papers the idea of the MFTM [1], the principle of operation [2-4], the first experimental set-up [5] and the first experimental results [6], the analysis of the optical system and some new experiments with the improved set-up [7] have been described. In this paper we continue to analyse the optical system. We give the analysis of the images of dot-like and straight line objects and show how the MFTM can be obtained from a traditional optical microscope by continuous modification of the latter.

2. THE POINT SPREAD FUNCTION OF THE MFTM

In order to clear up the character of the transformation of the optical information in the METM, let us start from a traditional optical microscope. By using the double diffraction principle of the image formation [8] any optical microscope can be converted into the optical arrangement shown in Fig.1 which is a typical one for Fourier Optics [10]. Let the input objects in thick layer of nuclear research emulsion be illumi-

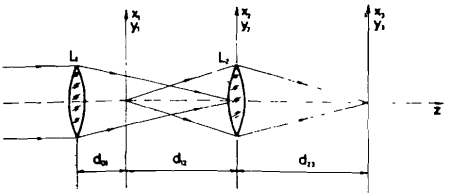

Fig.1. The Fourier Optics configuration of a traditional optical microscope.

nated by a convergent beam of coherent light crossover of which is in the Fourier plane (x_2, y_2). The lens L_1 executes a Fourier transformation of the input object described by the amplitude transmittance function $f(x_1, y_1)$ and the amplitude of the electric field $E(x_2, y_2)$ in the plane (x_2, y_2) can be written in the form of [10]

$$E(x_2, y_2) = \text{Const} \cdot \iint_{-\infty}^{\infty} f(x_1, y_1) \times \exp\left[-\frac{2\pi i}{\lambda d_{12}}(x_1 x_2 + y_1 y_2)\right] dx_1 dy_1 , \qquad /1/$$

where λ is the wave length of light, Const is a constant factor which can be henceforth omitted. The lens L_2 accomplishes a second Fourier transformation if the imaging condition

$$d_{12}^{-1} + d_{23}^{-1} = f_2^{-1} , \qquad /2/$$

is fulfilled where f_2 is the focal length of the lens L_2. The amplitude of the electric field $E(x_3, y_3)$ in the plane (x_3, y_3) is defined by the expression

$$E(x_3, y_3) = \iint_{-\infty}^{\infty} E(x_2, y_2) \times \exp\left[-\frac{2\pi i}{\lambda d_{23}}(x_2 x_3 + y_2 y_3)\right] dx_2 dy_2 , \qquad /3/$$

and gives an enlarged (d_{23}/d_{12} times) image of the input objects.

Now let us submit the lens L_2 to the following modifications. We add a mesooptical element [11] to the lens L_2. The mesooptical element consists of a negative conical lens, i.e. a plane-parallel disk from which a cone is removed. The optical system thus obtained is the basic scheme of the MFTM (Fig.2).

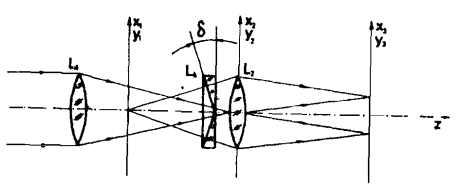

Fig.2. The basic configuration of the Mesooptical Fourier Transform Microscope (MFTM) with negative conical mesooptical element.

The complex amplitude transmittance function of the mesooptical element is given in [7] and has the form

$$t(x_2, y_2) = \exp[i\Delta\Phi(x_2, y_2)] . \qquad /4/$$

The phase shift $\Delta\Phi(x_2, y_2)$ over the plane-conical mesooptical element is equal within the Fourier optics approximation to

$$\Delta\Phi(x_2, y_2) = \frac{2\pi}{\lambda}(n-1)\operatorname{tg}\delta\sqrt{x_2^2 + y_2^2} = \frac{2\pi}{\lambda}\kappa\sqrt{x_2^2 + y_2^2} , \qquad /5/$$

where n is the refraction index of light inside the mesooptical element, δ is the taper angle shown in Fig.2 and κ the parameter of the conicity of the mesooptical lens L_2.

The amplitude at the output plane (x_3, y_3) for this case is

$$E(x_3, y_3) = \iint_{-\infty}^{\infty} E(x_2, y_2) \cdot \exp\left[\frac{2\pi i}{\lambda}\kappa\sqrt{x_2^2 + y_2^2}\right] \times \exp\left[-\frac{2\pi i}{\lambda d_{23}}(x_2 x_3 + y_2 y_3)\right] dx_2 dy_2 , \qquad /6/$$

where $E(x_2, y_2)$ is defined by Eq.(1). From Eqs.(6) and (1) we can see that any translation of the input objects in the plane (x_1, y_1) causes a corresponding translation of the output images in the plane (x_3, y_3). Due to this property the MFTM is a space invariant system [10]. To find out the point spread function [12] of the MFTM we introduce the polar coordinates

$$\left.\begin{aligned} r_i &= \sqrt{x_i^2 + y_i^2} , \\ \phi_i &= \operatorname{arctg}(y_i / x_i) , \end{aligned}\right\} \quad i = 1,2,3 \qquad /7/$$

and place a pinhole described by the δ-function $\delta(r_1)$ into the origin of the coordinates (x_1, y_1). Taking into account the axial symmetry of the whole system Eq.(6) can be written as

$$E(r_3) = \int_0^{\infty} r_2 \exp\left[\frac{2\pi i}{\lambda}\kappa r_2\right] \cdot J_0\left(\frac{2\pi r_2 r_3}{\lambda d_{23}}\right) dr_2 , \qquad /8/$$

where J_0 is the Bessel function of the zero order. By use of the Fourier theorem of the derivative of the Fourier transform /10/ and the relation /13/

$$\int_0^\infty \exp(ipx)\, J_0(cx)\, dx = \tag{9}$$

$$= \begin{Bmatrix} 1 \\ i \end{Bmatrix} (c^2 - p^2)^{-1/2} \begin{cases} 0 \le p < c, \\ 0 < c \le p, \end{cases}$$

we can get the point spread function of the MFTM as a function of the parameter of conicity κ:

$$E(r_3) = \begin{cases} -\kappa [(\kappa d_{23})^2 - r_3^2]^{-3/2}, & r_3 < \kappa d_{23}, \\ \kappa [r_3^2 - (\kappa d_{23})^2]^{-3/2}, & r_3 > \kappa d_{23}. \end{cases} \tag{10}$$

The amplitude of the light at the output plane of the MFTM is shown in Fig.3.

In the case when $\kappa = 0$ we have a traditional imaging system with the point spread function equal to $E(r_3) = \delta(r_3)$. This follows from Eq.(10) at $\kappa \to 0$. For $\kappa > 0$ the point spread function has the form of a bright focal circle with the radius $R = \kappa d_{23}$ and with the intensity light distribution around this circle which decreases as $|r_3 - R|^{-3}$. The effective width of this focal ring is determined by the entrance angular aperture of the mesooptical system. In ptinciple we can construct an ideal focal ring if the amplitude transparence of the mesooptical element has the form

$$t(r_2) = J_0(\frac{2\pi}{\lambda} \kappa r_2). \tag{11}$$

In this case the amplitude at the output plane /12/ is expressed as follows:

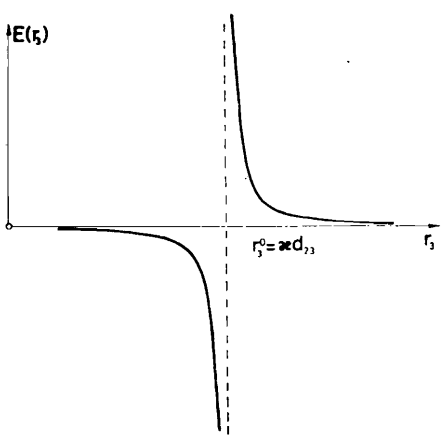

Fig.3. The amplitude light distribution near the focal circle of the MFTM.

$$E(r_3) = \int_0^\infty r_2 J_0(\frac{2\pi}{\lambda} \kappa r_2) \cdot J_0(\frac{2\pi r_2 r_3}{\lambda d_{23}})\, dr_2 = \tag{12}$$

$$= \text{Const.}\, \delta(r_3 - \kappa d_{23}).$$

3. THE IMAGE OF A STRAIGHT LINE SEGMENT IN MFTM

The most adequate objects for the MFTM are straight line segments which describe that part of the straight line particle tracks which occurs in the field of view of the MFTM. For the purpose of lucid explanation of image formation of these objects in the MFTM we have to follow the continuous conversion of the traditional optical microscope into the MFTM. This conversion has been modelled by computer through gradual increasing of the parameter of conicity κ. Some results of this computer simulation are given in Fig.4-6 in the form of 3D-plots where 2D-light intensity distributions over the outplane of the MFTM are presented.

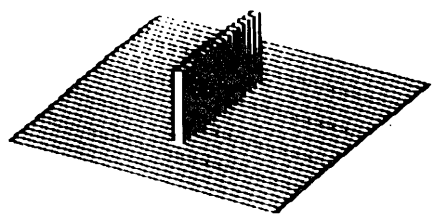

Fig.4. 3D-plot of the 2D-light intensity distribution in the image of a straight line segment produced by a traditional optical microscope.

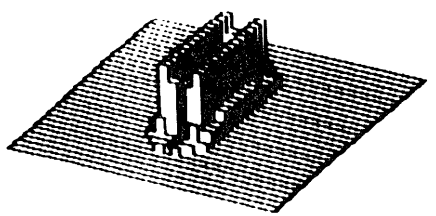

Fig.5. 3D-plot of the 2D-light intensity distribution in the mesooptical image of the same object as in Fig.4 produced by configuration in Fig.2 at a small conicity.

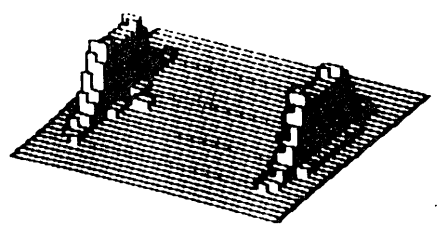

Fig.6. 3D-plot of the 2D-light intensity distribution of two output images in the MFTM for the same object as in Figs.4 and 5 at a greater conicity.

In the case of zero conicity we have a traditional image of a straight line segment (Fig.4). When the parameter of conicity κ increases the image is splitting in two image with a dark domain between them (Fig.5). On continuing this process we get images typical for the MFTM (Fig.6). The distance between two output signals is equal to the diameter of the focal circle. We can see that each particle track is transformed by the MFTM into two signals having the form of small spots lying on the focal ring and on the straight line perpendicular to the direction of the particle track.

The detailed analysis of two images thus produced or simply two output signals at the output plane of the MFTM for particular conditions of nuclear research emulsion was presented in [7]. In real experimental conditions we have $\mathcal{D}/w \geq 10^2$ and $w \approx 0{,}5-2\ \mu$m, where $\mathcal{D}$ is the diameter of the field of view of the MFTM and w is the width of the particle track. In this case the light distribution in the Fourier plane is practically concentrated within a narrow strip $2\lambda d_{12}/D$ wide and $2\lambda d_{12}/w$ long. The direction of this narrow strip is perpendicular to the direction of the particle track. Due to this property we can easily calculate the light intensity distribution at the output plane of the MFTM. It has been shown that the width of the output signal along the radial coordinate is defined by the factors which determine the width of the radial ring (§2). Thus in terms of the Rayleigh criterion [14] for the optical system with diffraction limited resolution the radial width of the output signals is equal to

$$\Delta\rho = \lambda/\alpha_{1/2} \qquad (13)$$

and determined by the total angular aperture $2\alpha_{1/2}$. The sagittal (angular) lenght of the output signals or its length along the tangent to the focal circle is given by Eq.(11) from [7]:

$$\Delta\ell_\theta = Dd_{23}/d_{12} = MD, \qquad (14)$$

where M is the linear magnification of the whole mesooptical system. The angular resolution $\Delta\theta$ of the MFTM is equal to

$$\Delta\theta = \Delta\ell_\theta/\pi R. \qquad (15)$$

In the MFTM design described in [5] we can obtain principally the radial resolutions $\Delta\rho \approx 1-2\ \mu$m and the angular, resolution $\Delta\theta \approx 5'-10'$.

The authors wish to thank S.A.Bunjatov for continuous interest and support and Yu.A.Batusov for useful disscussions of this paper.

REFERENCES

1. Soroko L.M. JINR publication, B1-13-81-229, Dubna, 1981.
2. Lyucov V.V., Soroko L.M. JINR publication, B1-13-81-312, Dubna, 1981.
3. Soroko L.M. JINR publication, B1-10-82-808, Dubna, 1982.
4. Soroko L.M. JINR publication, B1-10-82-809, Dubna, 1982.
5. Astakhov A.Ya. et al., Communication of JINR, P13-83-119, Dubna, 1983.
6. Astakhov A.Ya., Soroko L.M., Communication of JINR, P13-83-120, Dubna, 1983.
7. Astakhov A.Ya. et al. Communication of JINR, P13-84-277, Dubna, 1984.
8. Bencze Gy.L., Soroko L.M., JINR preprint, E13-84-310, Dubna, 1984.
9. Marechal A. and Francon M. Diffraction, Editions de la Revue d'Optique, Paris, 1960.
10. Goodman J.W. Introduction to Fourier Optics, McGraw-Hill, 1968.
11. Soroko L.M. Communication of JINR, D1-82-642, Dubna, 1982.
12. Papoulis A. Systems and Transforms with Applications in Optics, McGraw-Hill, 1968.
13. Прудников А.П. и др. Интегралы и ряды. Специальные функции. М.: Наука, 1983, p.185.
14. Born M., Wolf E. Principles of Optics, Pergamon Press, 2nd ed., 1964.

Received by Publishing Department
on June 5, 1987.

SUBJECT CATEGORIES OF THE JINR PUBLICATIONS

Index	Subject
1.	High energy experimental physics
2.	High energy theoretical physics
3.	Low energy experimental physics
4.	Low energy theoretical physics
5.	Mathematics
6.	Nuclear spectroscopy and radiochemistry
7.	Heavy ion physics
8.	Cryogenics
9.	Accelerators
10.	Automatization of data processing
11.	Computing mathematics and technique
12.	Chemistry
13.	Experimental techniques and methods
14.	Solid state physics. Liquids
15.	Experimental physics of nuclear reactions at low energies
16.	Health physics. Shieldings
17.	Theory of condenced matter
18.	Applied researches
19.	Biophysics

Бенце Д., Сороко Л.М.
E13-87-388

Изображающие свойства мезооптического фурье-микроскопа для ядерной фотоэмульсии

Преобразование оптического сигнала в мезооптическом фурье-микроскопе /МФМ/ для ядерной фотоэмульсии рассмотрено в терминах фурье-оптики. Прослежен непрерывный переход традиционного оптического микроскопа в мезооптический фурье-микроскоп. Обсуждаются изображения точечных объектов в виде прямых линий, которые дает мезооптический фурье-микроскоп.

Работа выполнена в Лаборатории ядерных проблем ОИЯИ.

Сообщение Объединенного института ядерных исследований. Дубна 1987

Bencze Gy.L., Soroko L.M.
E13-87-388

Imaging Properties of the Mesooptical Fourier Transform Microscope for Nuclear Research Emulsion

The optical signal transformation in the Mesooptical Fourier Transform Microscope (MFTM) for nuclear emulsion is treated in terms of Fourier Optics. A continuous conversion of the traditional optical microscope into the MFTM is followed. The images of dot-like and straight line objects given by the MFTM are discussed.

The investigation has been performed at the Laboratory of Nuclear Problems, JINR.

Communication of the Joint Institute for Nuclear Research. Dubna 1987